Rico, M., Bruix, M., Santoro, J., Gonzalez, C., Neira, J. L., Nieto, J. L., & Herranz, J. (1989) *Eur. J. Biochem. 183*, 623–638.
Robertson, A. D., Purisima, E. O., Eastman, M. A., & Scheraga, H. A. (1989) *Biochemistry 28*, 5930–5938.
Roder, H., Wagner, G., & Wüthrich, K. (1985) *Biochemistry 24*, 7407–7411.
Schmid, F. X., & Blaschek, H. (1984) *Biochemistry 23*, 2128–2133.
Shakhnovich, E. I., & Finkelstein, A. V. (1989) *Biopolymers 28*, 1667–1680.
Shoemaker, K. R., Fairman, R., York, E. J., Stewart, J. M., & Baldwin, R. L. (1988) in *Peptides: Chemistry and Biology* (Marshall, G. R., Ed.) pp 15–20, ESCOM, Leiden.
Strehlow, K. G., Robertson, A. D., & Baldwin, R. L. (1991) *Biochemistry 30*, 5810–5814.
Talluri, S., & Scheraga, H. A. (1990) *Biochem. Biophys. Res. Commun. 172*, 800–803.
Tanford, C. (1968) *Adv. Protein Chem. 23*, 121–282.
Tsong, T. Y., Hearn, R. H., Wrathall, D. P., & Sturtevant, J. M. (1970) *Biochemistry 9*, 2666–2677.
Udgaonkar, J. B., & Baldwin, R. L. (1988) *Nature 335*, 694–699.
Wagner, G. (1983) *J. Magn. Reson. 55*, 151–156.
Wedin, R. E., Delepierre, M., Dobson, C. M., & Poulsen, F. M. (1982) *Biochemistry 21*, 1098–1103.
Wlodawer, A., Borkakoti, N., Moss, D. S., & Howlin, B. (1986) *Acta Crystallogr. B42*, 379–387.

DNA Triplex Formation of Oligonucleotide Analogues Consisting of Linker Groups and Octamer Segments That Have Opposite Sugar–Phosphate Backbone Polarities†

Akira Ono,‡ Ching-Nien Chen,§ and Lou-sing Kan*,‡

Department of Biochemistry, School of Hygiene and Public Health, The Johns Hopkins University, 615 North Wolfe Street, Baltimore, Maryland 21205, and Biomedical Engineering & Instrumentation Program, NCRR, NIH, Bethesda, Maryland 20892

Received January 16, 1991; Revised Manuscript Received May 22, 1991

ABSTRACT: The DNA oligomer analogues 3′d(CTTTCTTT)5′-P4-5′d(TTCTTCTT)3′ (IV), 5′d-(TTTCTTTC)3′-P2-3′d(CTTTCTTT)5′ (V), and 5′d(TTTCTTTC)3′-P2-3′d(CTTTCTTT)5′-P4-5′d-(TTCTTCTT)3′ (VI) (P2= **P*P** and P4= **P*P*P*P**, where **P** = phosphate and ***** = 1,3-propanediol) have been synthesized. These oligomers consist of a linker group or groups and homopyrimidine oligonucleotides which have opposite sugar–phosphate backbone polarities. These oligomer analogues are designed to form triplexes with a duplex, 5′d(AAAGAAAGCCCTTTCTTTAAGAAGAA)3′·5′d(TTCTTCTTAAA-GAAAGGGCTTTCTTT)3′ (I), which contains small homopurine clusters alternately located in both strands. The length of the linker groups, P2 and P4, was based upon a computer modeling analysis. Triplex formation by the unlinked octamers 5′d(TTCTTCTT)3′ (II) and 5′d(TTTCTTTC)3′ (III) and the linked oligomer analogues IV–VI with the target duplex was studied by thermal denaturation at pH 5.2. The order of stabilities of triplex formation by these oligomers was I–V ≫ I–IV > I–(II, III). The mixture of I and VI showed two transitions corresponding to the dissociation of the third strand. The higher transition corresponded to the dissociation of 3′–3′-linked octamer segments, and the lower one corresponded to the dissociation of 5′–5′-linked octamer segments. The T_m of the latter transition was higher than that of the I–IV triplex; thus the triplex formed by the 5′–5′-linked octamer segment was stabilized by the triplex formed by the 3′–3′-linked octamer segments in the I–VI triplex. Triplex formation of this system was also studied in the presence of ethidium bromide. Only the I–IV triplex and the part of triplex formed by the 5′–5′-linked oligomer segments in the I–VI triplex were stabilized in the presence of ethidium bromide, whereas the I–V triplex or the I–(II, III) triplex was not. In the presence of ethidium bromide, the three octamer segments in VI dissociated from the duplex I in a synergistic manner. Negative bands at 230–210 nm were detected in the CD spectra of I–(II, III), and I–IV, I–V, or I–VI at pH 5.2, indicating triplex formation. Addition of ethidium bromide to the mixtures of oligomers changed their CD spectra only slightly. These results are useful when considering the design of oligonucleotide analogues that can bind as third strands to DNA duplexes of higher complexity.

Triple-stranded nucleic acid helices (triplexes) whose triads are composed of residues from two homopyrimidine strands and one homopurine strand have been studied in systems consisting of RNA and/or DNA strands (Felsenfeld et al., 1957, 1967; Michelson et al. 1967). The third strand (i.e., the second pyrimidine strand) is located in the major groove of a normal Watson–Crick duplex. Thymines and N3-protonated cytosines (in acidic condition) in the third-strand form Hoogsteen-type hydrogen bonds with adenines and guanines, respectively (Lipsett et al., 1963; Howard et al., 1964; Thiele et al., 1971). Interestingly, the sugar–phosphate backbone polarity of the third strand is parallel to that of the homopurine strand (Arnott et al., 1976; Moser & Dervan,

† This work was supported in part by NCI (Grant 5 PO1 CA42762-04) and by DOE (Grant DE-FG02-88ER60636). Preliminary results have been presented at the 1990 ASBMB/AAI Annual Meeting, New Orleans, LA, June 1990.
* To whom correspondence should be addressed.
‡ The Johns Hopkins University.
§ NIH.

0006-2960/91/0430-9914$02.50/0

1987; Santos et al., 1989, Rajagopal & Feigon, 1989a,b).

Circular dichroism (CD) spectroscopy has been useful for monitoring triplex formation in polymer and oligomer systems (Lee et al., 1979; Gray et al., 1987; Xodo et al., 1990; Callahan et al., 1991; Ono et al., 1991). The generation of a large negative band in the short-wavelength region (<230 nm) caused by formation of a poly[d(C^+-T)·d(A-G)·d(C-T)] triplex was reported (Lee et al., 1979), and this negative band was confirmed in an oligonucleotide system with the same sequence (Kan et al., 1991). In addition, ethidium bromide is a well-known DNA binding dye whose fluorescence emission intensity is enhanced dramatically when intercalating into a DNA duplex. As this emission is reduced by the binding of a third strand to an existing duplex, ethidium bromide has been used as a probe to study triplex formation in DNA (Lee et al., 1979, 1984; Morgan et al., 1979; Xodo et al., 1990; Kan et al., 1991; Scaria & Shafer, 1991).

In recent years, studies of oligonucleotide-directed triplex formation have been of prime interest. Chemically synthesized oligonucleotides and their analogues have been used for biological and biochemical studies such as site-specific cleavage of DNA (Moser & Dervan, 1987; Povsic & Dervan, 1989; Francois et al., 1989a; Beal & Dervan, 1991; Strobel & Dervan, 1991), inhibition of DNA–protein binding (Maher et al., 1989; Francois et al., 1989b; Hanvey et al., 1990), inhibition of gene expression (Cooney et al., 1988), protection of UV-induced damage (pyrimidine dimerization) (Lyamichev et al., 1990), etc. However, target sequences in these studies are limited because homopurine clusters with fairly long chain lengths are required for stable triplex formation. Such homopurine clusters are not always found within biologically important sequences such as those involved in gene control, protein binding, etc. Therefore, the design of oligonucleotide analogues that are able to form triplexes not only with homopurine sequences but also with those of higher complexity is important in extending fully the biological applications of the triplex (Horne & Dervan, 1990).

As a first step toward increasing the target duplex complexity, we examine the triplex formation of oligonucleotide analogues with a model DNA duplex. This duplex (I) consists of small homopurine clusters in both strands, represented as $5'(Pu)_8(Py)_{10}(Pu)_8 3'\cdot 5'(Py)_8(Pu)_{10}(Py)_8 3'$ (Figure 1a). Three homopurine clusters are indicated by shadows. The purine bases in these clusters can hydrogen bond to the residues in three third-strand homopyrimidine octanucleotides, one 5′d-(TTCTTCTT)3′ (II) octanucleotide and two 5′d-(TTTCTTTC)3′ (III) octanucleotides (Figure 1b). Since these three small purine clusters are alternately located on either side of duplex I, the third strands must bind separately with alternate duplex strands. Triplex formation of short third strands with these homopurine clusters may not be stable. However, their binding may be enhanced by linking these short homopyrimidine segments with an appropriate linker group or groups. This approach may induce cooperative binding interactions between the third-strand oligomer segments (Horne & Dervan, 1990).

Three linked oligomers were synthesized: a 5′–5′-linked oligomer 3′d(CTTTCTTT)5′-P4-5′d(TTCTTCTT)3′ (IV) (Figure 1c), a 3′–3′-linked oligomer, 5′d(TTTCTTTC)3′-P2-3′d(CTTTCTTT)5′ (V) (Figure 1d), and a doubly linked oligomer 5′d(TTTCTTTC)3′-P2-3′d(CTTTCTTT)5′-P4-5′d-(TTCTTCTT)3′ (VI) (Figure 1e) (P2= **P*P** and P4= **P*P*P*P**, where **P** = phosphate and ***** = 1,3-propanediol). These oligomers have opposite sugar–phosphate backbone polarities in different segments of the linear sequence, i.e., the

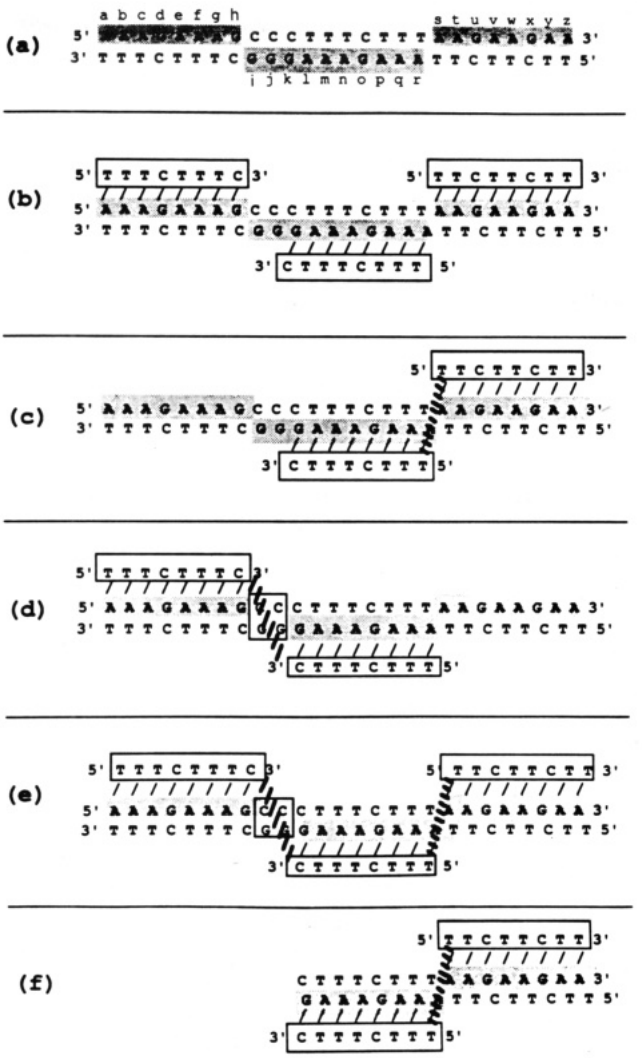

FIGURE 1: Binding schemes of the third strands with duplex I. (a) Sequence of duplex I. (b) Sequences of the unlinked homopyrimidine octamers used as the control third strands. Oligomer III, 5′d-(TTTCTTTC)3′, forms triplexes with homopurine clusters (indicated as abcdefg or rqponmlkj), and oligomer II, 5′d(TTCTTCTT)3′, forms a triplex with one homopurine cluster (indicated as stuvwxyz). (c) Binding scheme for the 5′–5′-linked oligomer IV with duplex I. 5′-Ends of octamer segments are linked by the P4 linker. (d) Binding scheme for the 3′–3′-linked oligomer V with duplex I. 3′-Ends of octamer segments are linked by the P2 linker. (e) Binding scheme for the doubly linked oligomer VI. 5′-Ends or 3′-ends of octamer segments are linked by P4 and P2, respectively. (f) Binding scheme for the 5′–5′-linked oligomer IV with duplex VII.

direction of the backbone is reversed at each linker site. Thus the polarity of each octamer segment is parallel to that of the corresponding homopurine cluster of duplex I as required for triplex formation. Two homopyrimidine octamers are linked between 5′-ends (5′–5′ linking) in oligomer IV, which binds with the 5′d(CTTTCTTTAAGAAGAA)3′·5′d-(TTCTTCTTAAAGAAAG)3′ region of duplex I [$5'(Py)_m$-$(Pu)_n 3'\cdot 5'(Py)_n(Pu)_m 3'$ type sequence] (Figure 1c). Two homopyrimidine octamers are linked between 3′-ends (3′–3′ linking) in oligomer V, which binds with the 5′d(AAA-GAAAGCCCTTTCTTT)3′·5′d(AAAGAAAGGGCTTT-CTTT)3′ region of duplex I [$5'(Pu)_m(Py)_l 3'\cdot 5'(Pu)_l(Py)_m 3'$ type sequence] (Figure 1d). In oligomer VI, three octamers are joined by two linkers, at the 5′–5′ and at the 3′–3′ linking sites, so that a triplex with the entire sequence of duplex I can be formed (Figure 1e). Additionally, a second duplex, 5′d-(CTTTCTTTAAGAAGAA)3′·5′d(TTCTTCTTAAA-GAAAG)3′ (VII), was designed to form a triplex with 5′–

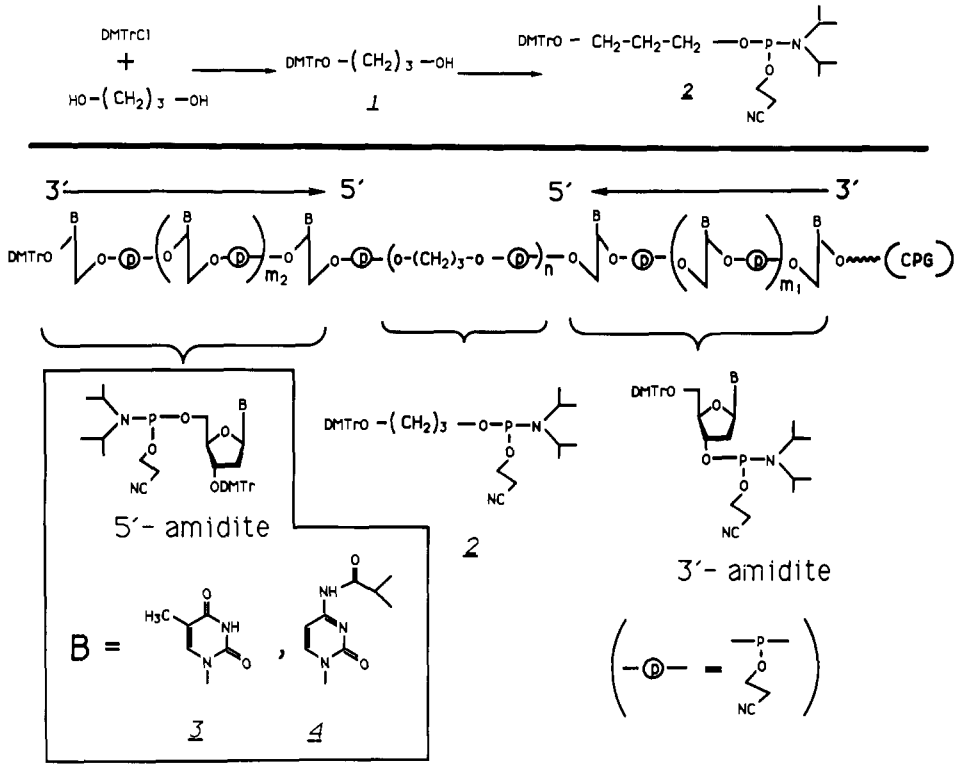

FIGURE 2: (Upper) Scheme for synthesis of the linker amidite **2**. (Lower) Scheme for synthesis of the 5′–5′-linked oligomer IV. Details are stated under Materials and Methods.

5′-linked oligomer IV (Figure 1f). In this system the extra duplex portion (cluster abcdefgh) of I + IV can be avoided.

In this report, the design of the linker groups for each linking site and the synthesis of the oligomer analogues are presented. Triplex formation of unlinked oligomers and their linked analogues with duplexes I and VII is studied by thermal denaturation and CD spectroscopy. The stability and conformation of the various triplexes are examined with and without the addition of ethidium bromide.

Materials and Methods

Molecular Graphics. The molecular graphics of triplexes with both 5′–5′-linked and 3′–3′-linked oligomers were generated by a MacroModel program (Interactive Molecular Modeling System V.3.0, Department of Chemistry, Columbia University, New York, NY) on a VAX 8600 computer. The coordinates of unit nucleotides in A form were adopted from fiber diffraction data for the poly(dA)·2[poly(dT)] triplex reported by Arnott and co-workers (Arnott et al., 1972). Graphics were generated and manipulated on an Evans & Sutherland PS390 workstation. No energy minimization was attempted during generation of the structures.

Synthesis of Amidite Synthons. All chemicals were obtained from Aldrich Chemical Co. (Milwaukee, WI). Solvents were obtained from Fisher Scientific Co. (Pittsburgh, PA). TLC was performed on silica gel $60F_{254}$ plates (Merck, Rahway, NJ) and column chromatography on silica gel G60 (70–230 mesh, ASMT, Merck).

HPLC was performed on a Vista 5500 (Varian, CA) with a PRP-1 column (Hamilton, Reno, NV). Snake venom phosphodiesterase I was obtained from Pharmacia (Piscataway, NJ).

Nuclear magnetic resonance (NMR) spectra were obtained on a Bruker WM-300 spectrometer. Chemical shifts are reported in parts per million (δ), and signals are described as s (singlet), d (doublet), t (triplet), or m (multiplet). Mass spectra (MS) were obtained on a BIO-ION Nordic (Uppsala, Sweden) BIN 10K time-of-flight mass spectrometer, equipped with a 10-mCi ^{252}Cf fission fragment ion source. Mass accuracy is about 0.1%.

Synthesis of O-(Dimethoxytrityl)-1,3-propanediol (**1**) (*Figure 2, Upper*). 1,3-Propanediol (1 mL, 13.8 mmol) and dimethoxytrityl chloride (340 mg, 1 mmol) were dissolved in pyridine (10 mL). The mixture was kept at 25 °C overnight, and then methanol (1 mL) was added. After 10 min, the solvent was evaporated in vacuo. The residue was partitioned between ethyl acetate and 5% $NaHCO_3$. The organic layer was collected and washed with water 5 times. After being dried over Na_2SO_4, the organic layer was concentrated to dryness in vacuo. The residue was chromatographed over a column of silica gel (3 cm i.d. × 12 cm) with *n*-hexane–ethyl acetate (1:1) as an eluent to give **1** as a gum (180 mg, 0.48 mmol, 48%): ^1H NMR (DMSO-d_6) δ 7.36–6.65 [13 H, m, aromatic protons of dimethoxytrityl (DMTr) group], 4.33 (1 H, t, OH), 3.71 (6 H, s, CH_3O), 3.50–3.42 (2 H, m, CH_2CH_2OH), 3.00 (2 H, t, DMTr-OCH_2CH_2), 1.73–1.64 (2 H, m $CH_2CH_2CH_2$); mass parent peak at *m/e* 379 (M^+).

Synthesis of Linker Amidite (**2**) (*Figure 2, Upper*). **1** was dried by coevaporation with anhydrous pyridine twice and then dissolved in CH_2Cl_2 (10 mL). *N,N*-Diisopropylethylamine (170 μL, 1.5 equiv) and 2-cyanoethyl *N,N*-diisopropylchlorophosphoramidite (130 μL, 1.2 equiv) (Sinha et al., 1983) were added. After 20 min, $CHCl_3$ and 5% $NaHCO_3$ were added to the solution, and the organic layer was collected and washed with water. After drying over Na_2SO_4, the organic layer was concentrated in vacuo. The residue was chromatographed over a column of silica gel (3 cm i.d. × 10 cm) with ethyl acetate as an eluent to give **2** as a viscous liquid (240 mg, 0.41 mmol, 86%): ^1H NMR (DMSO-d_6) δ 7.36–6.34 (13 H, m, aromatic protons of DMTr group), 3.72 (6 H, s, CH_3O), 3.70–3.44 [6 H, m, - CH_2OP and CH_2CH_2CN and $NCH(Me)_2$], 3.01–3.00 (2 H, m, DMTr-OCH_2), 2.66 (2 H, t, CH_2CN), 1.82–1.78 (2 H, m, $CH_2CH_2CH_2$), 1.09 (6 H, d, methyl protons of isopropyl group a), 1.01 (6 H, d, methyl

protons of isopropyl group b); mass parent peak at m/e 580 (M^+).

Synthesis of Thymidine 5'-Amidite (**3**) *and 2'-Deoxycytidine 5'-Amidite* (**4**) (*Figure 2, Lower*). 5'-Amidites **3** and **4** were synthesized according to a reported method (Sande et al., 1988).

Synthesis of Linked Oligonucleotides. The linked oligonucleotides IV–VI were synthesized on a DNA synthesizer (Milligen 7500) using solid support phosphoramidite triester chemistry (Beaucage et al., 1981; Sinha et al., 1983). A scheme for the synthesis of the oligomer IV or VI is shown in Figure 2, lower. Starting with a nucleoside attached on a solid support, the octamer segment 5'd(TTCTTCTT)3' was synthesized with a 3'-to-5' direction by using the 3'-amidites, and then the liner group P4 was elongated by consecutive couplings of **2** four times. Then, another octamer segment, 3'd(CTTTCTTT)5', was elongated with 5'-to-3' direction by using the 5'-amidites **3** and **4** (Sande et al., 1988). The oligomer VI was synthesized by a coupling of **2** and elongation of an octamer segment 5'd(TTTCTTTC)3' to the 3'-end of the oligomer IV. The octamer V was synthesized according to Horne and Dervan (1990). After being deblocked and cleaved from the solid support by concentrated NH_4OH treatment, oligomers protected with dimethoxytrityl (DMTr) groups were purified by HPLC. Fractions were treated with 80% acetic acid solution (deblocking the DMTr group), and then oligomers were purified by HPLC. All oligonucleotides of this preparation showed single peaks by HPLC analysis. Eleven OD units of IV, three OD units of V, and sixteen OD units of VI were obtained starting from 2 μmol of solid supporting materials. The extinction coefficients (ϵ, L·mol·strand^{-1}·cm^{-1}) of the oligonucleotides were determined by an enzymatic digestion method (Miller et al., 1980) as follows; II, 53 800; III, 53 800; 5'd(AAAGAAAGCCCTTTCTTTAAGAAGAA)3', 193 900; 5'd(TTCTTCTTAAAGAAAGGGCTTTCTTT)3', 180 200; 5'd(TTCTTCTTAAAGAAAG)3', 149 600; and 5'd(CTTTCTTTAAGAAGAA)3', 147 600. The extinction coefficients of IV (107 600), V (107 600), and VI (161 400) are the sum of the ϵ of their components (II and III).

UV Spectroscopy. UV absorbances were measured on Varian DMS 100 and Varian 219 spectrophotometers. Thermally induced transitions for each mixture of the oligomers was monitored by the Varian 219 with a thermoregulated sample compartment. Sample temperature was controlled by fluid circulating from a temperature-regulated bath monitored with a calibrated thermistor probe inserted in a "dummy" cuvette.

Solutions for thermal denaturation studies contain 3 μM of each oligomer in buffer (0.01 M sodium acetate, 0.75 M NaCl, 5 mM $MgCl_2$, pH 5.2) except for the mixture of the duplex I and the unlinked oligomers, which contained 3 μM duplex I, 3 μM II, and 6 μM III. Thermal transitions for each mixture were monitored by measuring the UV absorption at 260 nm in the absence or in the presence of ethidium bromide (3 or 6 μM).

CD Spectroscopy. CD spectra were obtained on a Jasco 500A CD spectropolarimeter (Tokyo, Japan). Buffer and sample conditions were the same as those used for the melting studies. CD spectra were also measured with or without 3 μM ethidium bromide. Sample temperature was controlled at 3 °C by using a circulating water bath.

Results

Design of the Linker Groups. In order to design appropriate linker groups for 5'–5' and 3'–3' linking sites, we examined

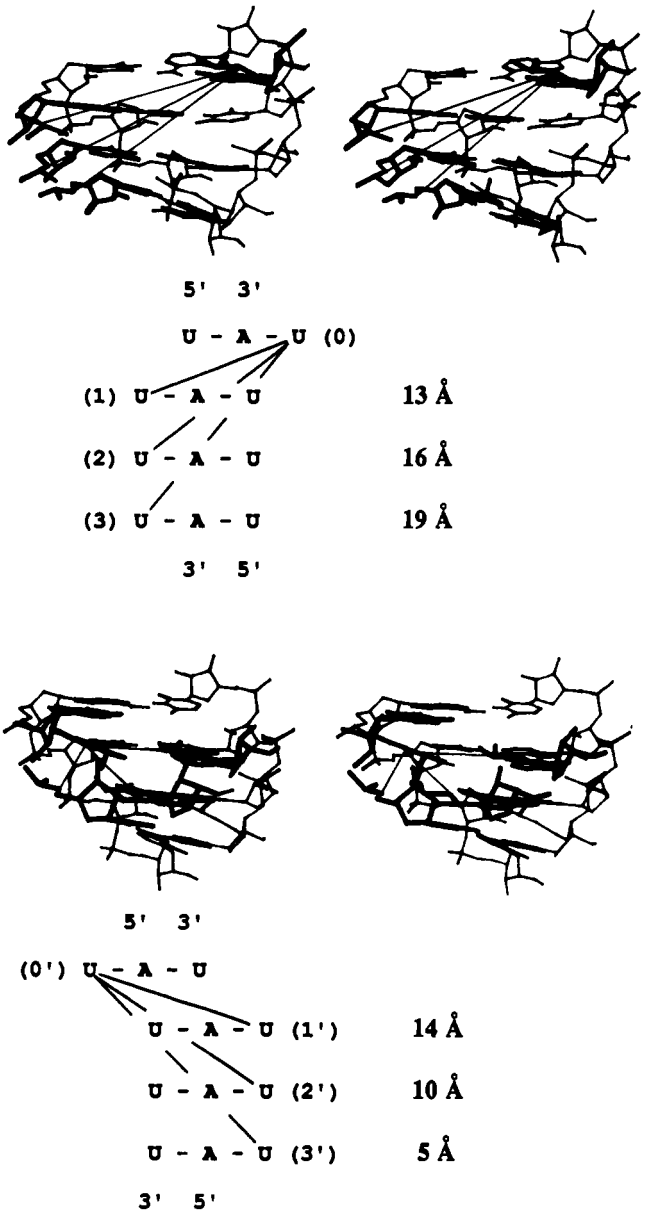

FIGURE 3: Stereoviews for the 5'–5' (upper) and 3'–3' (lower) linking sites in a triplex. Details are stated under Results.

the three-dimensional conformations of triplexes by computer graphics. Several research groups (Arnott et al., 1976; Santos et al., 1989) have reported that the duplex portion in a triplex is in an A-like conformation. Therefore, we studied the three-dimensional locations of the 5'-ends or 3'-ends of two third strands at the 5'–5' and the 3'–3' linking sites on A-type (RNA) helices (Figure 3). In this case, RNA duplexes are substitutions for DNA duplexes in an A-type conformation.

A model for the 5'–5' linking site is shown in stereoview in the upper part of Figure 3. This model consists of a tetraribonucleotide duplex, 5'r(UAAA)3'·5'r(UUUA)3', and four uridine monophosphates (UMPs) which are positioned so as to bind with adenines by Hoogsteen type hydrogen bonds in the major groove of the duplex. This duplex is a model for those consisting of the 5'$(Py)_n(Pu)_m$3'·5'$(Py)_m(Pu)_n$3' sequence, and the UMPs (numbered 0–3) represent possible positions for the 5'–5'-linked third strand. The distances between the 5'-oxygens of UMP(0) and UMP(1), 13 Å, UMP(0) and UMP(2), 16 Å, or UMP(0) and UMP(3), 19 Å, are calculated. These numbers correspond to the distances between 5'-ends of the third strands which are separated by zero, one,

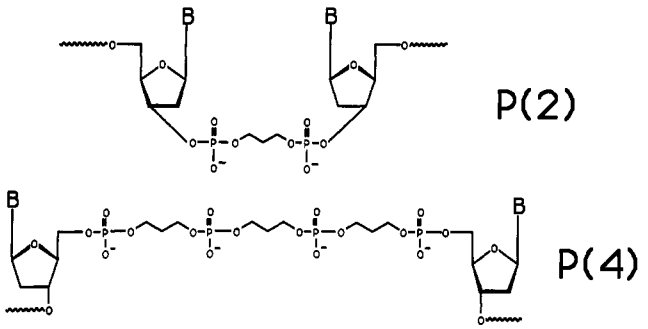

FIGURE 4: Structures of the P2 and P4 linker groups.

or two base pairs of duplex region.

A model for the 3′–3′ linking sites on a RNA duplex is given in Figure 3, lower portion. The tetraribonucleotide duplex is a model for those consisting of the 5′(Pu)$_l$(Py)$_m$3′·5′(Pu)$_m$-(Py)$_l$3′ sequence, and the four UMPs represent possible positions for 3′–3′-linked third strands. Distances between 3′-oxygen atoms of UMPs are regarded as the approximate distances between 3′-ends of the third strands. The distance between 3′-ends of UMP(0′) and UMP(3′) (5 Å), where there are two base pairs of intervening duplex region, is shorter than the distance between the UMP(0′) and the UMP(1′) (14 Å), where there is no such intervening region, or the distance between the UMP(0′) and the UMP(2′) (10 Å), where there is one intervening duplex base pair.

As discussed above, distances between the 5′-ends of the third strands are much longer than those between the 3′-ends. Also, close inspection of Figure 3 shows that the two hydroxyl groups of the 5′-ends are pointing in opposite directions. The linker group P4 consisting of four phosphates and three 1,3-propanediols (Figure 4) was therefore chosen to link the 5′-ends of third strands. The estimated length of such a segment should be in the range of 17–23 Å.

It is interesting to note that, at the 3′–3′ linking site, the ends of the third strands are very close together and that their locations are quite favorable for linking when there is a gap of two base pairs of duplex region. Therefore, we designed the 3′–3′-linked oligomer IV to allow for two base pairs of intervening duplex reigon (indicated by the open squares in Figure 1d,e) on a target sequence (Horne & Dervan, 1990). The linker group P2 consisting of two phosphates and one 1,3-propanediol (Figure 4) was estimated to have a suitable length (5–8 Å) for this kind of linkage.

Table I: Melting Temperatures of Dissociations of the Third Strands from Duplexes in the Presence or Absence of Ethidium Bromide

duplex + third strands	T_m (°C) at ethidium bromide		
	0 μM	3 μM	6 μM
I + II	26		
I + III	26		
I + II, III	26		27
I + IV	27	37	38
I + V	52		50
I + VI			
5′–5′-linked octamer segments	34	49	50
3′–3′-linked octamer segments	47	49	50
VII + II, III	26	25	
VII + IV	28	37	37

Studies of Triplex Formation by Thermal Denaturation. In order to study the effect of these linker groups on triplex formation, we examined the stability of triplexes formed by the oligomers II–VI with the target duplex I by thermal denaturation in the buffer at pH 5.2. In Figure 5, graphs of relative UV absorbance with respect to temperature (A–D) and the corresponding first derivative curves (a–d) are shown.

A transition (T_m = 71 °C) corresponding to the melting of the duplex I appeared in all thermal denaturation profiles (Figure 5). All mixtures in a buffer of 0.01 M Tris-HCl, 0.75 M NaCl, and 5 mM $MgCl_2$ at pH 7.8 showed only one transition (T_m = 72 °C) corresponding to the melting of duplex I (data not shown). Therefore, lower transitions detected in the mixtures containing duplex I and any third strands at pH 5.2 correspond to the dissociations of third strands from duplex I. These T_m's are listed in Table I.

Dissociations of unlinked octamer II or III or the mixture of II and III from the duplex I showed the same T_m's (26 °C, Table I); thus unlinked octamers II and III did not show any cooperative binding. The T_m of the dissociation of the 5′–5′-linked oligomer IV (27 °C) from the duplex I is slightly higher than that of the unlinked octamers (26 °C). Also the shape of the transition for the dissociation of IV is sharper than that for the dissociation of II and III, indicating that the linked oligomer may have more cooperative binding. In contrast, T_m of the dissociation of the 3′–3′-linked oligomer V (52 °C) is significantly higher than that for the dissociations of the unlinked octamers or for the 5′–5′-linked oligomer IV.

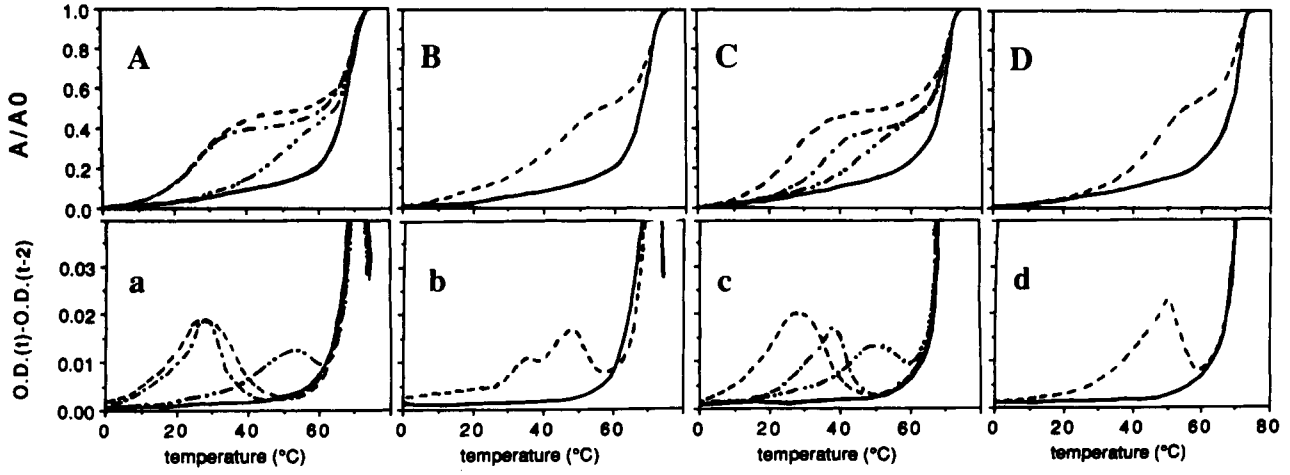

FIGURE 5: Profiles of UV absorption versus temperature (upper case) and corresponding first derivative curves (lower case). (A, a) (—) Duplex I; (---) I + unlinked octamers; (-·-) I + the 5′–5′-linked oligomer IV; (-··-) the 3′–3′-linked oligomers V and I. (B, b) (—) Duplex I; (---) I + the doubly linked oligomer VI. (C, c) (—) Duplex I with 6 μM ethidium bromide; (---) I + II + III with 6 μM ethidium bromide; (-·-) I + IV with 3 μM ethidium bromide; (-··-) I + V with 6 μM ethidium bromide. (D, d) (—) Duplex I with 6 μM ethidium bromide; (---) I + VI with 3 μM ethidium bromide.

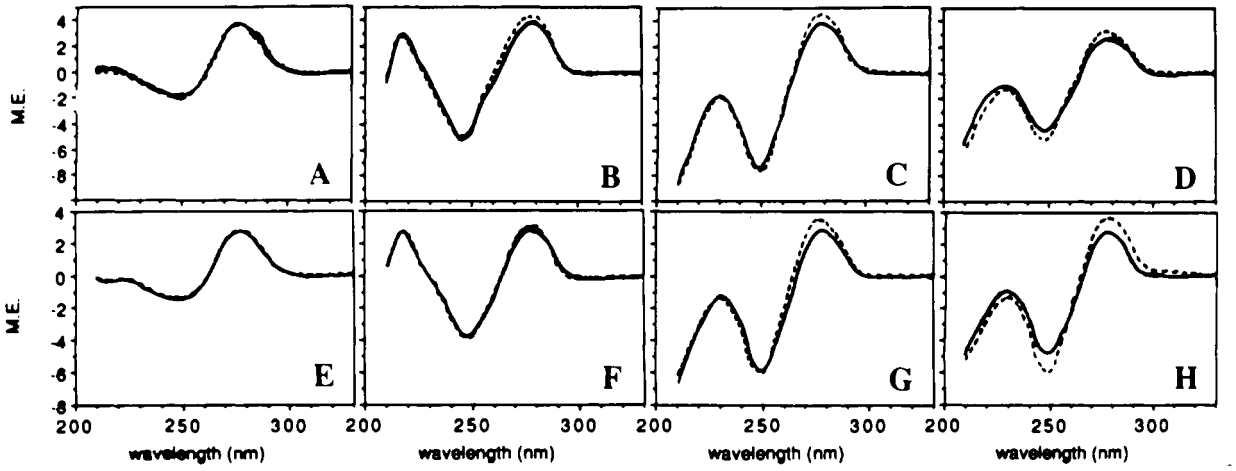

FIGURE 6: CD spectra. (A) (—) VI; (---) VI + ethidium bromide (1:1); (-·-) II + III (1:2); (-··-) II + III + ethidium bromide (1:2:1). (B) (—) Duplex I; (---) I + ethidium bromide (1:1). (C) (—) I + II + III (1:1:2); (---) I + II + III + ethidium bromide (1:1:2:1). (D) (—) I + VI (1:1); (---) I + VI + ethidium bromide (1:1:1). (E) (—) IV; (---) IV + ethidium bromide (1:1); (-·-) II + III (1:1); (-··-) II + III + ethidium bromide (1:1:1). (F) (—) VII; (---) VII + ethidium bromide (1:1). (G) (—) VII + II + III (1:1:1); (---) VII + II + III + ethidium bromide (1:1:1:1). (H) (—) VII + IV (1:1); (---) VII + IV + ethidium bromide (1:1:1). Molar ellipticity (M.E. × 10^5) is shown per single strand (A and E) or per duplex (B–D and F–H). CD spectra were measured at 3 °C in 0.01 M sodium acetate, 0.75 M NaCl, and 5 mM $MgCl_2$ at pH 5.2.

As shown in Figure 5B, the mixture of VI and the duplex I showed two transitions corresponding to dissociation of the third strand. The higher transition (48 °C) which is closest to that observed for the dissociation of the 3′–3′-linked oligomer V alone (52 °C) is attributed to the dissociation of the 3′–3′-linked octamer segments [5′d(TTTCTTTC)3′-P2-3′d-(CTTTCTTT)5′]. The lower transition (T_m = 34 °C) would then correspond to the dissociation of the 5′–5′-linked oligomer segment [3′d(TTCTTCTT)5′-P4-] bound on to the stuvwxyz region (Figure 1e). This T_m is higher than that for the dissociation of IV; thus this result indicates that triplex formation of the 5′–5′-linked octamer segment is stabilized by the neighboring 3′–3′-linked octamer segments.

As shown in Figure 5C and Table I, the T_m for the dissociation of the 5′–5′-linked oligomer IV from the duplex I increased by 10 °C in the presence of 1 equiv (3 μM) of ethidium bromide. Addition of 2 equiv (6 μM) of the dye did not show further stabilization. This stabilization by the dye detected in the triplex formation for the 5′–5′-linked oligomers was not found for the unlinked oligomers or for the 3′–3′-linked oligomer V (Figure 5a, Table I). Therefore, this stabilization is proposed to be caused by a specific interaction between the dye and the 5′–5′-linked sites. Furthermore, we studied the effect of the dye on stabilization of the triplex formed by IV with duplex VII which does not have any residual duplex region upon binding of the 5′–5′ linker oligomer (Figure 1f). As shown in Table I, T_m's of the dissociation of IV from the duplex VII in the presence of the dye are almost identical with those from the duplex I. This result clearly shows that the duplex region of the I–VI complex has no effect in stabilization of triplex formation by the dye.

Ethidium bromide also stabilized the triplex formation of the 5′–5′-linked oligomer segment of doubly linked oligomer VI with the duplex I. In the presence of the dye, the mixture of VI and I showed only one transition corresponding to the dissociation of the third strand (Figure 5d). Triplex formation by the 5′–5′-linked octamer segments was stabilized in the presence of ethidium bromide as detected in the triplex formation of the 5′–5′-linked oligomer IV with I or VII. In addition, the triplex formation by 5′–5′-linked octamer segments could again be stabilized by the neighboring triplexes formed by the 3′–3′-linked octamer segments. As a result of these cooperative effects, the three octamer segments dissociated synergistically in a single transition.

CD Spectra. The 5′–5′-linked oligomer IV, the doubly linked oligomer VI, and the mixtures of the unlinked octamers II and III showed similar CD spectra (Figure 6A,E). The duplexes I and VII showed similar spectra (Figure 6B,F), which are typical of duplexes in a B-type conformation. On the other hand, triplexes formed by unlinked octamers or by linked oligomers with target duplex I or VII showed large negative bands between 230 and 210 nm (Figure 6C,D). These bands are not observed in the spectra of the duplexes or in those of the third strands. The presence of a negative band below 230 nm has been shown to be indicative of triplex formation (Lee et al., 1984, Callahan et al., 1991; Kan et al., 1991).

CD spectra of the VII–IV triplex (Figure 6H) and the VII–(II, III) triplex (Figure 6G) are similar. The most notable difference is that the intensity of the negative bands at 250 and 210 nm of the latter spectrum is slightly larger than those of the former spectrum. On the other hand, the spectra of the I–IV triplex (Figure 6D) and of the I–(II, III) triplex (Figure 6C) show similar splitting patterns and positions of the positive and the negative bands, except that the intensities of both the positive and the negative bands of the latter spectrum are greater than those of the former spectrum.

Addition of ethidium bromide did not cause any obvious changes in the CD spectra of the third strands (Figure 6A,E) and the duplexes (Figure 6B,F). On the other hand, the intensity of positive and negative bands of CD spectra of triplexes was increased, but only slightly, upon addition of the dye. These alterations in intensities showed similar tendencies for triplexes formed by unlinked octamers (Figure 6C,G) or by linked oligomers (Figure 6D,H). Thus addition of the dye did not result in large conformational alterations of the triplexes formed by 5′–5′-linked oligomer IV, even though the dye highly and specifically stabilized the triplex formation by IV.

Discussion

Design of Linker Groups. Since several research groups (Arnott et al., 1976; Santos et al., 1989) have reported that the duplex portion in a triplex is in an A-like conformation, we studied the three-dimensional locations of the 5′-ends or 3′-ends of two third strands at the 5′–5′ and the 3′–3′ linking

sites on A-type (RNA) helices. However, sugar moieties in N-conformer have been found in triplexes by recent NMR studies (Rajagopal & Feigon, 1989a,b; Sklenar & Feigon, 1990). Therefore, we also studied the three-dimensional locations on B-type duplex system. However, each 5′–5′ or 3′–3′ linking site on A-type helices or on B-type helices showed similar tendencies for the geographical relationship between 5′-ends or between 3′-ends of third strands. Therefore, only the computer graphics with A-type (RNA) duplexes are shown in this report (Figure 3).

One of the most impressive results of the modeling study was found at the 3′–3′ linking site, in which 3′-ends are closest to each other when a gap of two base pairs of duplex region is introduced between the 3′-ends. This feature is due to the helical aspect of the duplex and the placement of the third-strand residues within the major groove (Figure 3, lower). In keeping with this result, the 3′–3′-linked oligomer V was designed to allow for two base pairs of intervening duplex region (indicated by the open squares in Figure 1d,e) on a target sequence (Horne & Dervan, 1990). The result that the I–V triplex is more stable than the unlinked parent triplex (Table I) also shows the appropriateness of the design of the P2 linker (Figure 4). Also, in conformity to the result that the distances between 5′-ends are longer than those observed for 3′-ends, a longer linker, P4 (Figure 4), was designed for the 5′–5′ linking. Efficiencies of both linker groups and features of both linked sites are discussed in more detail below.

Triplex Formation of the Linked Oligomers with the Duplexes I and VII. 5′–5′ linking shows no obvious stabilization of triplex formation (Figure 5 and Table I). Since the CD spectrum of the mixture of the 5′–5′-linked oligomer IV and the duplex VII (Figure 6H) and that of the mixture of II, III, and VII (Figure 6G) are similar to each other, it is expected that the conformation of the former is similar to that of the latter. Therefore, the P4 linker must be long enough to link two third strands without causing significant distortions in the conformation of the triplex. However, the P4 linker did not stabilize triplex formation efficiently. One of the causes of this may be that highly concentrated negative charges (phoshates) in the P4 linker destabilize triplex formation since a triplex already has an excess of negative charges in three sugar–phosphate backbones which repel each other. This energetic disadvantage may nullify any cooperative advantages caused by linking of two third strands, resulting in the inefficiency of 5′–5′ linking for stabilization of triplex formation.

On the other hand, the intensity of the CD spectrum of the mixture of the doubly linked oligomer VI and the duplex I (Figure 6D) is smaller than that of the mixture of the unlinked II, III, and duplex I (Figure 6C). This observation may be the result of conformational differences between the triplex formed by 3′–3′-linked octamer segments with duplex I and the conformation of the unlinked parent triplex. As the CD spectrum of the triplex formed by the 5′–5′-linked oligomer IV and VII is quite similar to that of the triplex formed by II, III, and VII (Figures 1f and 6G,H), the additional segment of duplex I bound by the 3′–3′-linked third strand (cluster abcdefgh, Figure 1a) and the linking site itself is inferred to be the origin of this alteration in structure. The overall spectral features of the two triplexes are similar but of different magnitudes; therefore, some conformational differences are implied. The 3′–3′-linked site is the major structural feature which could account for this change. It is possible that this site has a different structure, e.g., bent or shifted in base stacking, from that of the unlinked parent triplex. Even though the magnitude of the I–VI CD spectrum is less than that observed for the I–(II, III) triplex (Figure 6C,D) the stability of the 3′–3′-linked segment is significantly greater than that observed for the unlinked parent triplex. Therefore, the altered conformation of this linked site may afford greater stability to the triple-stranded complex. Conversely, as the 5′–5′ linking did not stabilize the triplex formation over that observed for the unlinked parent triplex, the conformation in this linked site can be assumed to be very similar to the parent triplex. This is confirmed by the CD observations (Figure 6G,H).

It is worthwhile to note that the triplex formed by the 5′–5′-linked octamer segment of the doubly linked oligomer VI was stabilized by the neighboring triplex formed by the 3′–3′-linked octamer segments (Figure 5B and Table I). This observation can be extended to triplex formation with DNA regions consisting of more complicated sequences represented as $5'(Pu)_l(Py)_m(Pu)_n\cdots(Py)_z3'$ using the multiply linked oligomer analogues as third strands. If less stable linked regions (i.e., 5′–5′-linked regions) can be cooperatively and energetically compensated for by more stable flanking regions, triplex formation may be optimized.

Stabilization of Triplex Formation by Ethidium Bromide. As the emission of ethidium bromide is reduced by the binding of a third strand to an existing duplex, the dye was used as a probe to study triplex formation in DNA (Lee et al., 1979, 1984; Morgan et al., 1979; Xodo et al., 1990; Callahan, et al., 1991; Scaria & Shafer, 1991). Also, a fluorescence spectroscopic study indicated triplex formation in our linked oligomer system (data not shown). In addition, we found that triplex formation by IV with the duplex was stabilized in the presence of the dye (data not shown). Therefore, by thermal denaturation, we studied the effect of ethidium bromide for the stability of triplex formation of linked oligomers IV, V, VI or unlinked octamers II and III with the target duplex I and the target duplex VII which was designed to form a triplex with IV without possessing any duplex regions. Since addition of ethidium bromide highly stabilizes the triplex formed by the 5′–5′-linked oligomer IV (Figure 5C and Table I) but did not stabilize triplexes formed by unlinked octamers or by the 3′–3′-linked oligomer V (Figure 5C and Table I), it is inferred that the dye interacts only with the 5′–5′ linking site. This interaction between the dye and 5′–5′ linking site appears to be highly specific since 1 equiv of ethidium bromide is enough for the stabilization of triplex formation and increase of the dye concentration did not provide further stabilization (Table I). From these results, we propose that this stabilization effect by the dye is not caused by intercalation of the dye into the duplex region or into the triplex region of the complex of IV and I, but may be caused by interaction of the dye with the 5′–5′ linking site. Since addition of ethidium bromide did not largely change the CD spectrum of the triplex formed by the 5′–5′-linked oligomer IV and the duplex VII, interaction of the dye with the 5′–5′ linking site may not cause any large conformational alterations of the helix. From these observations, it is possible that the dye intercalates into the 5′-TA-3′ step at the 5′–5′ linking site. Also, the positive charge on the dye may help neutralize the negative charges on the P4 linker, resulting in a favorable interaction. These results suggest the potential value of using various combinations of linker groups and intercalating groups not only for the design of new linker systems but also for the design of new DNA binding compounds.

Conclusion

We have shown that the third-strand analogues consisting of a linker (or linker groups) and homopyrimidine oligomers which have various sugar–phosphate backbone polarities can

form stable triplexes with two or more homopurine segments located on opposite sides of a target duplex. CD spectra of the triplexes showed negative bands at 230–210 nm, indicating triplex formation. The entire triple helix consisting of short third-strand segments and homopurine clusters can be stabilized by cooperative triplex formation between third-strand segments when they are appropriately linked. These observations can be expanded to triplex formation with DNA regions consisting of more complicated sequences represented as $5'(Pu)_l(Py)_m(Pu)_n\text{---}(Py)_z3'$. Also the observation that triplex formation of 5′–5′-linked oligomers was stabilized in the presence of ethidium bromide suggests the potential value of using various combinations of linker groups and intercalating groups for the design of new linker systems.

ACKNOWLEDGMENTS

Dr. Paul O. P. Ts'o is the Principal Investigator and Program Director of the two grants listed in the title footnote. We thank him for his suggestions and discussions of this project. We are indebeted to Rong Wang for measuring the mass spectra and to the Middle Atlantic Mass Spectrometry Laboratory, The Johns Hopkins University, an NSF Regional Instrumentation Facility established by NSF Grant DIR-86-10589. We also thank the NCI ASCL group at Frederick, MD, for providing the computing facilities used in molecular modeling. NMR spectra were obtained at the Biochemistry NMR Facility Center established by NIH Grant GM 27512. We thank Dr. S. K. Yang for providing the CD spectrometer. Finally, we thank Ms. Tina L. Trapane for helpful discussion and excellent editorial assistance.

REFERENCES

Arnott, S., Hukins, D. W., & Dover, S. D. (1972) *Biochem. Biophys. Res. Commun. 48*, 1392–1399.

Arnott, S., Bond, P. J., Selsing, E., & Smith, P. J. C. (1976) *Nucleic Acids Res. 3*, 2459–2470.

Beal, P. A., & Dervan, P. B. (1991) *Science 251*, 1360–1363.

Beaucage, S. L., & Caruthers, M. H. (1981) *Tetrahedron Lett. 22*, 1858–1862.

Callahan, D. E., Trapane, T. L., Miller, P. S., Ts's, P. O. P., & Kan, L.-S. (1991) *Biochemistry 30*, 1650–1655.

Cooney, M., Czernuszewicz, G., Postel, E. H., Flint, S. J., & Hogan, M. E. (1988) *Science 241*, 456–459.

Felsenfeld, G., & Miles, T. (1967) *Annu. Rev. Biochem. 36*, 407–448.

Felsenfeld, G., Davies, D. R., & Rich, A. (1957) *J. Am. Chem. Soc. 79*, 2023–2024.

Francois, J.-C., Saison-Behmoaras, T., Barbier, C., Chassignol, M., Thuong, N. T., & Helene, C. (1989a) *Proc. Natl. Acad. Sci. U.S.A. 86*, 9702–9706.

Francois, J.-C., Saison-Behmoaras, T., Thoung, N. T., & Helene, C. (1989b) *Biochemistry 28*, 9617–9619.

Hanvey, J. C., Shimizu, M., & Wells, R. D. (1990) *Nucleic Acids Res. 18*, 157–161.

Horne, D. A., & Dervan, P. B. (1990) *J. Am. Chem. Soc. 112*, 2435–2437.

Howard, F. B., Frazier, J., Lipsett, M. N., & Miles, H. T. (1964) *Biochem. Biophys. Res. Commun. 17*, 93–102.

Kan, L.-S., Callahan, D. E., Trapane, T. L., Miller, P. S., Ts'o, P. O. P. (1991) *J. Biomol. Struct. Dyn. 8*, 911–933.

Lee, J. S., Johnson, D. A., & Morgan, A. R. (1979) *Nucleic Acids Res. 6*, 3073–3091.

Lipsett, M. N. (1963) *Biochem. Biophys. Res. Commun. 11*, 224–228.

Lyamichev, V. I., Frank-Kamenetskii, M. D., & Soyfer, V. N. (1990) *Nature 344*, 568–570.

Maher, L. J., III, Wold, B., & Dervan, P. B. (1989) *Science 245*, 725–730.

Michelson, A. M., Massoulie, J., & Guschlbauer, W. (1967) *Prog. Nucleic Acid Res. Mol. Biol. 6*, 83–141.

Miller, P. S., Cheng, D. M., Dreon, N., Jayaraman, K., Kan, L.-S., Leutzinger, E. E., Pulford, S. M., & Ts'o, P. O. P. (1980) *Biochemistry 19*, 4688–4698.

Morgan, A. R., Lee, J. S., Pulleyblank, D. E., Murray, N. L., & Evans, D. H. (1979) *Nucleic Acids Res. 7*, 547–568.

Moser, H. E., & Dervan, P. B. (1987) *Science 238*, 645–650.

Pilch, D. S., Brousseau, R., & Shafer, R. H. (1990) *Nucleic Acids Res. 18*, 5743–5750.

Povsic, T. J., & Dervan, P. B. (1989) *J. Am. Chem. Soc. 111*, 3059–3061.

Rajagopal, P., & Feigon, J. (1989a) *Nature 339*, 637–640.

Rajagopal, P., & Feigon, J. (1989b) *Biochemistry 28*, 7859–7870.

Santos, C., Rosen, M., & Patel, D. (1989) *Biochemistry 28*, 7282–7289.

Scaria, P. V., & Shafer, R. H. (1991) *Biophys. J. 59*, (2), 415a.

Sinha, N. D., Biernat, J., & Koster, H. (1983) *Tetrahedron Lett. 24*, 5843–5846.

Sklenar, V., & Feigon, J. (1990) *Nature 345*, 836–838.

Strobel, S. A., & Dervan, P. B. (1991) *Nature 350*, 172–174.

Thiele, D., & Guschlbauer, W. (1971) *Biopolymers 10*, 143–157.

van de Sande, J. H., Ramsing, N. B., Germann, M. W., Elhorst, W., Kalisch, B. W., Kitzing, E. V., Pon, R. T., Clegg, R. C., & Jovin, T. M. (1988) *Science 241*, 551–557.

Xodo, L. E., Manzini, G., & Quadrifoglio, F. (1990) *Nucleic Acids Res. 18*, 3557–3564.